Design of Paper Path Detection and Diagnostic System in Ink-Jet Printers Using an Observer-Based Technique

Kuan-Heng Chen and Syh-Shiuh Yeh

Abstract—**As the speed of paper feeding processes in an ink-jet printer is increased, the paper feeding mechanisms are usually prone to induce some paper transport problems such as paper jamming and slipping, and some mechanical problems such as gear cracking and chattering. Therefore, for ensuring printing qualities and for preventing destructive damages, the paper path detection in ink-jet printers is required. In this paper, we explore the feasibility of using speed perturbation observer to detect paper path situations in an ink-jet printer. Moreover, in comparing with the existing approaches, this paper presents an approach without additional sensors. The speed perturbation observer composed of a nominal plant, a low-pass filter, and an identification unit is developed to detect paper path situations during paper feeding processes. The design concept is based on the fact that external disturbances usually significantly affect the speed performances of an axial mechanical system. Since the paper feeding processes in ink-jet printers are equivalent to that the interaction among paper and paper feeding mechanisms exerts external disturbances on the driven motor, it is interesting to detect paper path situations by estimating speed perturbations induced by different paper feeding actions. The proposed approach is implemented on an ink-jet printer and two usual paper path situations are tested. The experimental results demonstrate that the proposed approach can accurately respond to the different paper path situations caused by different paper feeding actions.**

Index Terms—**paper path, detection and diagnostic, ink-jet printers, observer-based technique**

I. Introduction

INK-jet printers are widely used in our living environment. However, as ink-jet printers operate under higher speeds, the paper feeding mechanisms are usually more prone to induce some problems. Although well-designed paper feeding mechanisms [1, 2] and well-controlled paper feeding systems [3-5] can provide reliable and stable paper feeding processes, some problems may occur and limit the running performances for a long period using an ink-jet printer including paper sticking, jamming, and slipping. Some mechanical factors may also provide adverse effects on paper feeding processes including gear cracking, chattering, and wearing. Therefore, it is important to detect paper path situations during paper feeding processes for ensuring printing qualities and for preventing destructive damages.

Some researchers have proposed several approaches that can be applied to detect paper path situations in ink-jet printers. Zhao et al. [6] proposed a model-based monitoring and fault diagnosis method to efficiently detect and isolate incipient and abrupt faults in paper printing machines. In addition to the built-in sensors, audio and current sensors are deployed to detect fourteen paper path situations including paper jamming, paper slipping, gear cracking, and so on. Although the experimental results validate their approach, many sensors deployed for detecting paper path situations increases the production cost of an ink-jet printer. Fung et al. [7] proposed a fault detection method to detect cartridge situations in ink-jet printers by applying neural networks and the motor fault detection scheme proposed by the authors. Although their approach can be applied to detect different paper path situations in ink-jet printers, the computation complexity of neural networks makes their approach difficult to be implemented on an embedded system with limited computation resources. In practice, many sensors are usually added to paper feeding mechanisms for sensing and detecting paper path situations [8, 9]. However, those approaches may have some problems including:

- one sensor usually detects only one paper path situation in real applications;
- many sensors in an ink-jet printer substantially increase the production cost;
- the setup of sensors increases the design complexity of paper feeding mechanisms;
- many sensors usually increase the difficulty in maintaining an ink-jet printer.

Therefore, it is desired to design a paper path detection method that uses few sensors and has little computation complexity. In this paper, based on the following two facts:

- external disturbances usually significantly affect the speed performances of an axial mechanical system; and
- the paper feeding processes in an ink-jet printer are equivalent to that the interaction among paper and paper feeding mechanisms exerts external disturbances on the driven motor,

the speed perturbation observer is designed to detect different

Manuscript received May 12, 2012. This work was supported in part by the National Science Council of the Republic of China under Contract NSC 100-2221-E-027-009 and the Industrial Technology Research Institute, ROC, under project number 9353C72000, which is subcontracted from the Ministry of Economic Affairs, ROC.

K. H. Chen is with the Institute of Mechatronic Engineering, National Taipei University of Technology, Taiwan (phone: +886-2-2771-2171; fax: +886-2-2731-7191; e-mail: khchen@ntut.edu.tw).

S. S. Yeh is with the Department of Mechanical Engineering, National Taipei University of Technology, Taiwan (phone: +886-2-2771-2171; fax: +886-2-2731-7191; e-mail: ssyeh@ntut.edu.tw).

paper path situations induced by different paper feeding actions.

The design of the speed perturbation observer is derived from the design of the torque disturbance observer. In recent years, the disturbance observer is widely applied to motion control systems for observing external disturbances. Katsura et. al. [10, 11] proposed the acceleration based control with the disturbance observer such that the force servoing and the position regulator can be integrated in the acceleration control loop for developing a medical forceps system. Yasui et. al. [12] proposed an adaptive disturbance observer design and applied to engine speed control such that the control system provided accurate and rapid engine speed control under all engine conditions. Liu and Svoboda [13] proposed the integrated controller combined with sliding-mode fuzzy neural network, feedback-error-learning strategy, and nonlinear disturbance observer for improving the precision of the tracking control. Chen [14] proposed a general framework with nonlinear disturbance observer for improving disturbance attenuation ability of a two-link robotic manipulator. Yeh et. al. [15] proposed an integrated motion control design with digital disturbance observer for improving the contouring accuracy of multi-axis motion control systems. Kwon and Chung [16] proposed a discrete perturbation observer design in state-space for motion control applications. The effect of the Q-filter on performance and robustness is also discussed in the discrete-time domain. Bertoluzzo et. al. [17] further found that the stability of feedback control system with disturbance observer is closely related to the disturbance observer bandwidth, the current-loop bandwidth, the sampling time and the mismatch in the parameters. Although excellent performances are usually obtained, some problems still exist on the realization of the disturbance observer [17].

The first problem in implementing the disturbance observer is the need of acceleration signal. In the present research, the acceleration signal is obtained from the double differentiation of the position signal. However, the operation for double differentiation usually generates considerable noise superimposed on the acceleration signal and thus the low-pass filter with narrow bandwidth is required for noise attenuation. The low-pass filter with narrow bandwidth not only slows down the estimation of external disturbances but also deteriorates the transient robustness of control systems. The second problem in implementing the disturbance observer is the need of inverse dynamics. To precisely estimate the external disturbances, the inverse dynamics of the observed plant is applied to the design of disturbance observer. However, the observer using the inverse dynamics induces unstable computation for the discrete-time processing with improper sampling time. Although the digital disturbance observer design with nominal FIR filter proposed by Yeh and Hsu [15] provides stable computation for the discrete-time processing, the performance for estimating external disturbances is limited by the bandwidth of velocity control loop. Moreover, to precisely estimate the external torque disturbances, a current sensor is usually required in implementing the disturbance observer on an inkjet printer, and this requirement may increase the production cost. Considering the realization of disturbance observer, an observer design without acceleration signal and inverse dynamics is needed to exactly estimate external disturbances of an axial motion control system. Murakami et. al. [18] proposed a disturbance observer design with pseudo-differentiator for obtaining the angular acceleration signal. However, the observer design with the first-order low-pass filter can not efficiently isolate the adverse effects caused by noise perturbations.

In some applications, it is not critical for exactly estimating external disturbances. The observation of adverse effects caused by external disturbances is more important. Because external disturbances affect the speed performances of an axial motion system, the observation of speed variations induced by external disturbances is instead of the exact estimation of external disturbances for some control applications. Thus, Chen and Yeh [19] proposed the design of a speed perturbation observer to estimate the speed variations induced by external disturbances; moreover, in this paper, the speed perturbation observer is further applied to observe speed variations for detecting paper path situations induced by paper-feeding actions. In contrast with the torque disturbance observer, for implementing an observer on an ink-jet printer to detect paper path situations, the speed perturbation observer design uses the speed signal obtained from the single differentiation of position signal. Although the single differentiation operator generates noise superimposed on the speed signal, a conventional low-pass filter is applied to attenuate noise perturbations. The low-pass filter with suitable bandwidth provides good observing results and maintains the transient robustness of motion control systems. Moreover, the speed perturbation observer design does not use an inverse nominal plant model that may cause unstable computation in digital control systems. Because it is not required to precisely estimate the external torque disturbances in our approach, the speed perturbation observer does not use current sensor. Besides, since specific paper path situation usually exhibits some specific features on the observed perturbation signal, by using feature extraction and recognition algorithms, the identification unit included in the speed perturbation observer is developed to identify different paper path situations. Experimental results on an ink-jet printer demonstrate that the proposed approach can successfully identify paper jamming and mechanical chattering situations during paper feeding processes without additional sensors.

In detail, this paper is organized as follows. Section II presents the design of a speed perturbation observer for estimating the speed variations induced by external disturbances. Section III describes the design of a post-processing unit for reducing the adverse effects caused by modeling errors and measurement noises. The low-pass filter design and a disturbance isolation method are also mentioned in section III. Sections IV and V show some experimental results for evaluating the proposed approach on an ink-jet printer. Section VI concludes this paper.

II. Design of Speed Perturbation Observer

Considering the speed perturbation observer as shown in Fig. 1. T is the sampling time. $u^*(t)$ is the sampled driving

force from digital controller and $U^*(s)$ is the corresponding transformation in frequency domain. $\tau(t)$ is the torque command for driving servo systems. It's also the output signal of Zero-order-hold filter $H(s)$ with input signal $u^*(t)$. $T(s)$ is the corresponding transformation in frequency domain. $\tau_d(t)$ is the torque disturbance from environment. $\tau_d^*(t)$ is the sampled torque disturbance and $T_d{}^*(s)$ is the corresponding transformation in frequency domain. $w(t)$ is the rotating speed of servo motor and $W(s)$ is the corresponding transformation in frequency domain. $\theta(t)$ is the angular position of servo motor. $\delta^*(t)$ is the high frequency noise signal and $\Delta^*(s)$ is the corresponding transformation in frequency domain. $v^*(t)$ is the sampled rotating speed of servo motor and $V^*(s)$ is the corresponding transformation in frequency domain. The signal contains the high frequency noise signal $\delta^*(t)$. $d^*(t)$ is the estimated disturbance signal in discrete time domain and $D^*(s)$ is the corresponding transformation in frequency domain. $\hat{d}^*(t)$ is the output signal from digital low-pass filter $LPF(z^{-1})$ with estimated disturbance $d^*(t)$ as the input signal. $G(s)$ is the referred dynamic system. $H(s)$ is the zero-order-hold (Z.O.H) filter. $LPF(z^{-1})$ is the applied low-pass filter.

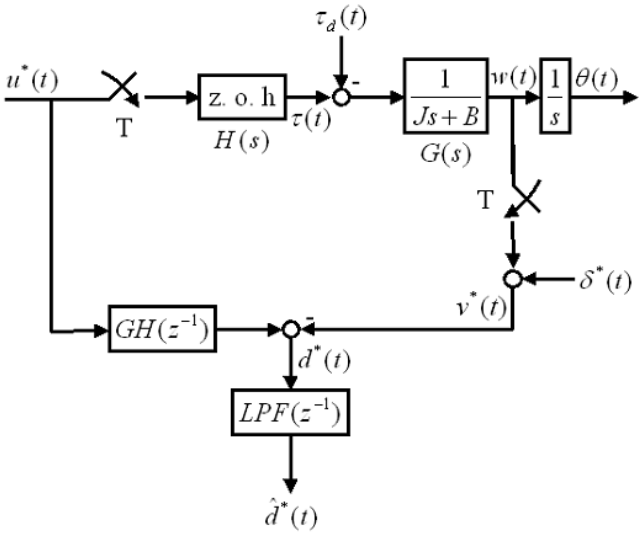

Fig. 1. The proposed discrete-time speed perturbation observer.

Since,

$$T(s) = U^*(s)H(s)$$

and

$$W(s) = G(s)[T(s) - T_d(s)] = G(s)H(s)U^*(s) - G(s)T_d(s)$$

The sampled rotating speed of servo motor without noise perturbation is obtained as

$$W^*(s) = L\{w^*(t)\} = GH^*(s)U^*(s) - GT_d{}^*(s)$$

and the sampled rotating speed of servo motor is thus obtained as

$$V^*(s) = W^*(s) + \Delta^*(s) = GH^*(s)U^*(s) - GT_d{}^*(s) + \Delta^*(s)$$

Therefore, the estimated disturbance signal is derived as

$$D^*(s) = GH^*(s)U^*(s) - V^*(s) = GT_d{}^*(s) - \Delta^*(s)$$

By applying the definition of the Z-transformation, the estimated disturbance signal is represented as

$$D(z^{-1}) = GT_d(z^{-1}) - \Delta(z^{-1}) \quad (1)$$

Equation (1) denotes the estimated disturbance signal $d^*(t)$ contains the filtered disturbance $GT_d(z^{-1})$ and high frequency noise signal $\delta^*(t)$. To degrade the adverse effects caused by high frequency noise signal $\delta^*(t)$, the low-pass filter is applied to the estimated disturbance signal $d^*(t)$. The filtered disturbance signal $\hat{d}^*(t)$ is thus obtained as

$$\hat{D}(z^{-1}) = LPF(z^{-1})GT_d(z^{-1}) - LPF(z^{-1})\Delta(z^{-1}) \quad (2)$$

where $\hat{D}(z^{-1})$ is the Z-transformation of the output signal $\hat{d}^*(t)$. For low-pass filter designed with suitable cutoff frequency, (2) can be rewritten as

$$\hat{D}(z^{-1}) \cong LPF(z^{-1})GT_d(z^{-1}) \quad (3)$$

Equation (3) denotes that the torque disturbance from environment could be estimated from observed signal $\hat{d}^*(t)$. Clearly, (3) denotes that the observed value $\hat{d}^*(t)$ is the filtered response of external disturbance $\tau_d(t)$. Fig. 2 shows the equivalent system of (3). As shown in Fig. 2, because $\hat{d}^*(t)$ is the low-pass filtered signal with input which is sampled from the output of dynamic system $G(s)$. Thus, the physical meaning of observed value $\hat{d}^*(t)$ is the same as $v^*(t)$ which is the sampled rotating speed of servo motor. Equation (3) implies the observed value $\hat{d}^*(t)$ responds to the fluctuation of rotating speed induced by external disturbance $\tau_d(t)$. Although the speed variation induced by external disturbances is observed by applying the observer as shown in Fig. 1, some topics must be further discussed for improving the performance of observer.

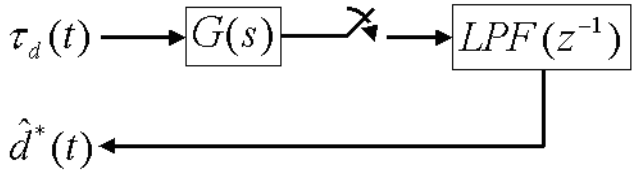

Fig. 2. The equivalent system of observed value $\hat{d}^*(t)$.

The discrete-time disturbance observer as shown in Fig. 1 is sensitive to the modeling error of dynamic system $G(s)$. A compensation algorithm is applied to design the speed variation observer such that the observer is robust to the modeling error of dynamic system. The low-pass filter $LPF(z^{-1})$ is applied to the disturbance observer for depressing the adverse effect caused by measurement noise. The cut-off frequency must be carefully concerned in designing low-pass filter such that the noisy signals from measurement process can be successfully isolated. The observer as shown in Fig. 1 can thus observe the speed

variation caused by external disturbances. For some control applications, a disturbance isolation method is needed to observe speed variation caused by specific disturbance. Therefore, a post processing unit design with suitable bandwidth of low-pass filter is required for reducing the adverse effects caused by modeling error and measurement noise, and for isolating the speed variation caused by specific disturbance.

III. The Post Processing Unit

In this paper, a post-processing unit is applied to further process the observed signal $\hat{d}^*(t)$ for improving the estimation of observer. The design consideration of low-pass filter is also mentioned at the end of the section.

A. Modeling error compensation

As shown in Fig. 1, by replacing filter $GH(z^{-1})$ with nominal filter $G_nH(z^{-1})$, the estimated disturbance signal $D^*(s)$ is obtained as

$$D^*(s) = G_nH^*(s)U^*(s) - V^*(s)$$

where, $G_n(s)$ is the nominal model of $G(s)$. It's usually obtained by regular system identification method. Because the sampled rotating speed of servo motor is derived as

$$V^*(s) = W^*(s) + \Delta^*(s) = GH^*(s)U^*(s) - GT_d{}^*(s) + \Delta^*(s)$$

The estimated disturbance signal $D^*(s)$ is rewritten as

$$D^*(s) = \left[G_nH^*(s) - GH^*(s)\right]U^*(s) + GT_d{}^*(s) - \Delta^*(s)$$

or

$$\begin{aligned} D(z^{-1}) &= \left[G_nH(z^{-1}) - GH(z^{-1})\right]U(z^{-1}) \\ &\quad + GT_d(z^{-1}) - \Delta(z^{-1}) \end{aligned} \tag{4}$$

Equation (4) represents the estimated disturbance signal in discrete-frequency domain. As shown in (4), (1) is obtained when the nominal model $G_n(s)$ is exactly the same as plant $G(s)$. By applying the low-pass filter as shown in Fig. 1, the observed value $\hat{D}(z^{-1})$ is obtained as

$$\begin{aligned} \hat{D}(z^{-1}) &= LPF(z^{-1})\left[G_nH(z^{-1}) - GH(z^{-1})\right]U(z^{-1}) \\ &\quad + LPF(z^{-1})GT_d(z^{-1}) - LPF(z^{-1})\Delta(z^{-1}) \end{aligned} \tag{5}$$

For low-pass filter designed with suitable cutoff frequency, (5) can be rewritten as

$$\begin{aligned} \hat{D}(z^{-1}) &\cong LPF(z^{-1})\left[G_nH(z^{-1}) - GH(z^{-1})\right]U(z^{-1}) \\ &\quad + LPF(z^{-1})GT_d(z^{-1}) \end{aligned} \tag{6}$$

Define the perturbation function $P_e(z^{-1})$ as

$$P_e(z^{-1}) = LPF(z^{-1})\left[G_nH(z^{-1}) - GH(z^{-1})\right] \tag{7}$$

Equation (6) can be further rewritten as

$$\hat{D}(z^{-1}) \cong P_e(z^{-1})U(z^{-1}) + LPF(z^{-1})GT_d(z^{-1}) \tag{8}$$

Based on the equivalent system as shown in Fig. 2, the modified equivalent system is shown as Fig. 3. A compensation algorithm for degrading the adverse effects caused by modeling error of dynamic system is proposed in this paper.

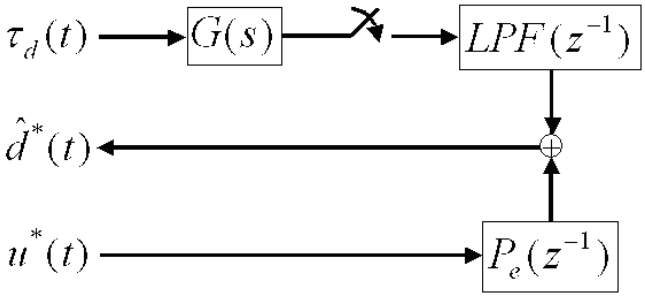

Fig. 3. The modified equivalent system.

Defining the compensation filter $\Omega(z^{-1})$ and the compensation structure as shown in Fig. 4, the value $\hat{D}(z^{-1})$ is obtained as

$$\begin{aligned} \hat{D}(z^{-1}) &\cong P_e(z^{-1})U(z^{-1}) + LPF(z^{-1})GT_d(z^{-1}) \\ &\quad - \Omega(z^{-1})U(z^{-1}) \end{aligned} \tag{9}$$

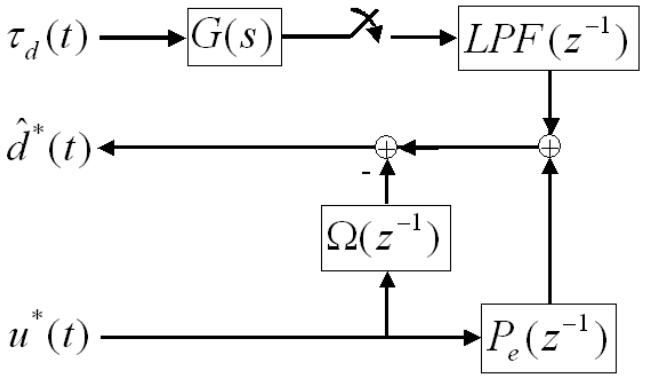

Fig. 4. The compensation structure.

Therefore, the goal for designing the compensation filter $\Omega(z^{-1})$ is to minimize the superior function as

$$\sup_{\omega}\left\|LPF(\omega)\left[G_nH(\omega) - GH(\omega)\right] - \Omega(\omega)\right\| \tag{10}$$

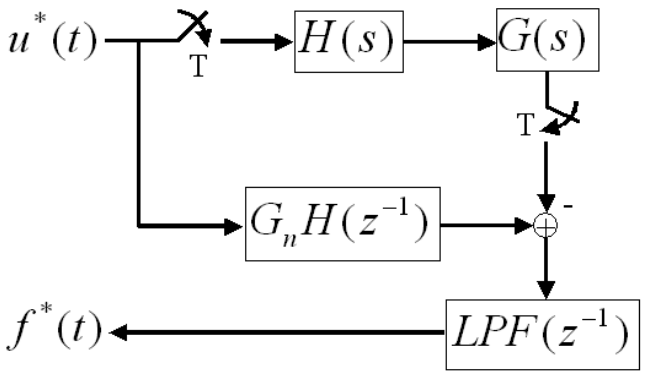

Fig. 5. The off-line identification structure.

In this paper, the off-line identification method is used to design the compensation filter. Fig. 5 shows the off-line identification structure. The compensation filter $\Omega(z^{-1})$ is obtained by applying the system identification algorithm with the excitation signal $u^*(t)$ and the corresponding output signal $f^*(t)$. The compensation structure shown in Fig. 4 reduces the adverse effects caused by modeling error. However, because the frequency responses of modeling error $\left[G_nH(z^{-1}) - GH(z^{-1})\right]$ are usually in higher frequency range,

the perturbation term $P_e(z^{-1})U(z^{-1})$ in (8) may be less significant by applying the low-pass filter $LPF(z^{-1})$ with suitable design of cut-off frequency.

B. Speed variation caused by specific torque disturbance

In general, the observer as shown in Fig. 1 observes the speed perturbation induced by external disturbances include the reaction torque when the mechanical system does the force task and the load torque caused by Coriolis force, centrifugal force, friction force, gravity force, and so on [19]. In practice, for some applications, only the speed perturbation induced by specific torque disturbance is the main concern in control systems. For instance, the observation of speed variation caused by reaction torque could be used to estimate the operating situation of mechanical systems that perform the force task with human. Usually, besides the speed variation induced by reaction torque, it is possible to identify the speed variation caused by specific load torque if some mechanical factors and motion properties are known in advance by implementing several motion tests. As shown in Fig. 6, the on-line compensation method is applied to distinguish the speed variation caused by different torque disturbances from the observed signal. $Co_f^*(t)$, $Ce_f^*(t)$, $Fr_f^*(t)$, and $Gr_f^*(t)$ denote the sampled load torque caused by Coriolis force, centrifugal force, friction force, and gravity force, respectively. The compensation function $LPFG_n(z^{-1})$ is obtained as

$$LPFG_n(z^{-1}) = LPF(z^{-1}) \cdot G_n(z^{-1})$$

where, $G_n(z^{-1})$ is the Z-transformation of the nominal plant $G_n(s)$. Similar to the load torque compensation proposed by Katsura [10] and Murakami [18], the speed variation caused by specific load torque is identified by compensating the speed variation caused by other load torque. For instance, for estimating the speed variation caused by reaction torque, the speed variation caused by load torque must be compensated as shown in Fig. 6. It is import to precisely estimate the sampled load torque $Co_f^*(t)$, $Ce_f^*(t)$, $Fr_f^*(t)$, and $Gr_f^*(t)$. The estimation is realizable by taking some identification processes.

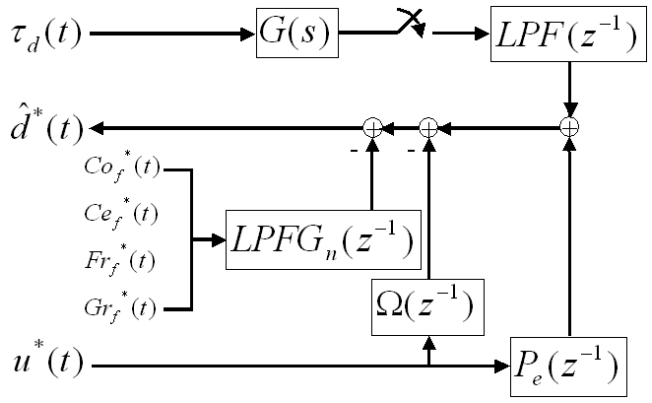

Fig. 6. The on-line compensation method.

C. Design consideration of low-pass filter

Similar to the disturbance observer, the low-pass filter is the central in speed perturbation observer design. Because the acceleration signal obtained from the double differentiation of the position signal is required in implementing the disturbance observer, the low-pass filter with narrow bandwidth usually slows down the disturbance estimation and deteriorates the transient robustness. In this paper, a speed perturbation observer design is proposed to estimate the speed variation induced by external disturbances. Because the speed signal obtained from the single differentiation of position signal is applied in implementing the observer, a conventional low-pass filter design with suitable bandwidth is employed to attenuate noise perturbations. The proposed observer design also provides good estimation results and maintains the transient robustness of control systems.

As shown in Fig. 1, the main concern in designing the low-pass filter $LPF(z^{-1})$ is for reducing the adverse effects caused by measurement noise. However, referring to the modified equivalent system as shown in Fig. 3, when the frequency responses of modeling error $\left[G_nH(z^{-1}) - GH(z^{-1})\right]$ are in higher frequency range, the low-pass filter design with suitable bandwidth reduces the perturbation $P_e(z^{-1})U(z^{-1})$ caused by modeling error. Thus, in this paper, the design of low-pass filter $LPF(z^{-1})$ is for reducing the adverse effects caused by measurement noise and modeling error. Fig. 7 shows the design concept of the low-pass filter in speed perturbation observer. By taking frequency analysis, the low-pass filter design with suitable bandwidth can attenuate perturbation caused by measurement noise and modeling error.

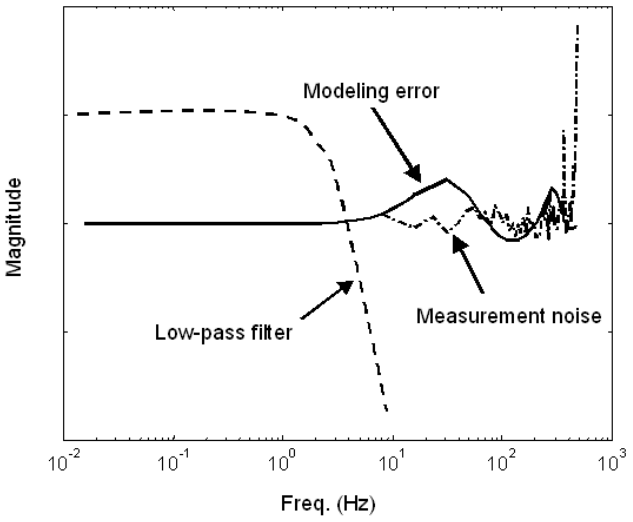

Fig. 7. The consideration for designing low-pass filter.

IV. Experimental Results: Axial Mechanical System

The experimental setup of an axial mechanical system for the present study is shown in Fig. 8. The applied motion control system consists of a personal computer, a DSP-based motion control card, and a mechanical system. The personal computer and DSP-based motion control card generated control commands and recorded signals, including: the input

commands for controllers, position outputs, and the driving forces for AC servo drivers. The DSP-based motion control card has built-in a high-performance TI TMS320C32 digital signal processor (DSP), which is capable of implementing some functions at a sampling period of 1 ms. The mechanical system is composed of a Panasonic AC servo motor, a gear set, and a handler. The mechanical system can do a force task when operator manually operates the handler that is built at the top of gear set. The experimental setup is an axial motion control system for testing the proposed speed disturbance observer.

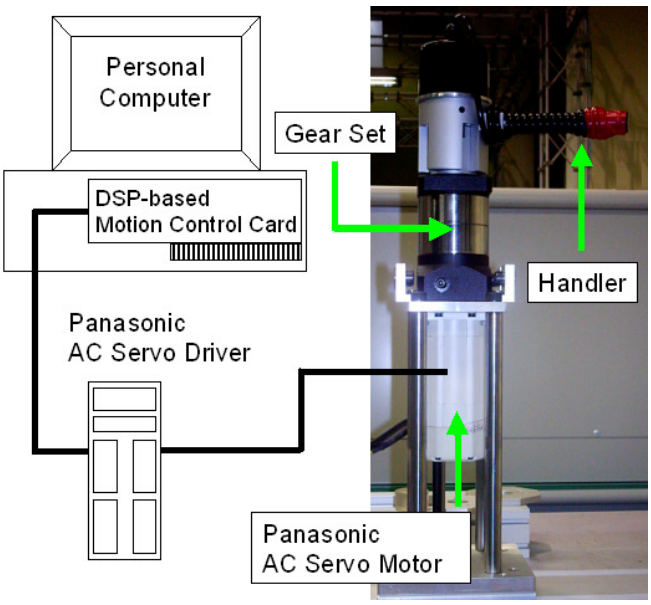

Fig. 8. The experimental setup of an axial mechanical system.

A. System identification

The torque equation of the axial mechanical system is written as

$$J_m\ddot{\theta}_m + B_m\dot{\theta}_m = T_m$$

where θ_m [rad] is the angular displacement, $\dot{\theta}_m$ [rad/sec] is the angular velocity, and $\ddot{\theta}_m$ [rad/sec^2] is the angular acceleration. J_m [$Nm/rad/sec^2$] denotes the equivalent inertia of the axial mechanical system. B_m [$Nm/rad/sec$] denotes the lumped viscous-friction coefficient. T_m [Nm] is the applied torque and R is the gear ratio. By applying the identification algorithm [20, 21], the system parameters (J_m, B_m) are obtained as

$$J_m = 0.000031369\ [Nm/rad/sec^2]$$

$$B_m = 0.00039\ [Nm/rad/sec]$$

$$R = 0.04$$

For testing the identified parameters, the step responses with different step input commands are compared in this paper. As shown in Fig. 9, the testing results show that the identified parameters are acceptable for designing the speed perturbation observer.

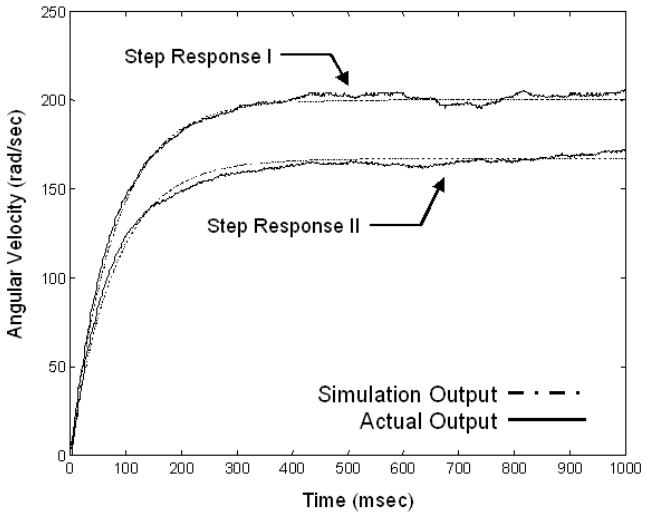

Fig. 9. Step responses of the axial mechanical system.

B. Frequency analysis of modeling error

Before designing the low-pass filter $LPF(z^{-1})$, frequency analysis of modeling error is performed for obtaining more design information in frequency domain. By applying the off-line identification as shown in Fig. 5, the frequency responses of modeling error before applying low-pass filter is shown in Fig. 10. The modeling error is enlarged after 3Hz. Therefore, to reduce the adverse effects caused by modeling error, the low-pass filter is designed with bandwidth less than 3Hz.

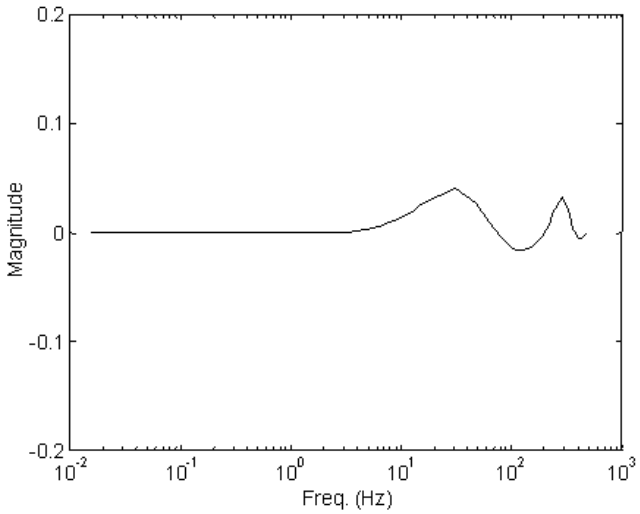

Fig. 10. The frequency response of modeling error.

C. Frequency analysis of measurement noise

The frequency analysis of measurement noise is performed before designing the low-pass filter $LPF(z^{-1})$. Fig. 11 shows the frequency responses of measurement noise. Obviously, the low-pass filter with bandwidth less than 4Hz is required for reducing the adverse effects caused by measurement noise.

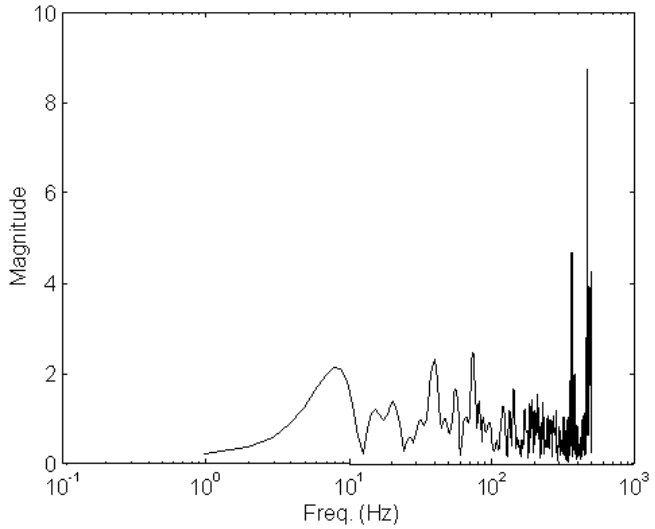

Fig. 11. The frequency response of measurement noise.

D. The low-pass filter design

According to the frequency analysis of modeling error and measurement noise, a 4th-order low-pass filter $LPF(z^{-1})$ is designed as

$$LPF(z^{-1}) = \frac{\begin{pmatrix} 0.0770 + 0.3080z^{-1} + 0.4619z^{-2} \\ + 0.3080z^{-3} + 0.0770z^{-4} \end{pmatrix} \times 10^{-7}}{1 - 3.9507z^{-1} + 5.8534z^{-2} - 3.8546z^{-3} + 0.9519z^{-4}} \quad (11)$$

Fig. 12 shows the frequency response of the designed low-pass filter. The bandwidth of the low-pass filter $LPF(z^{-1})$ is 3Hz.

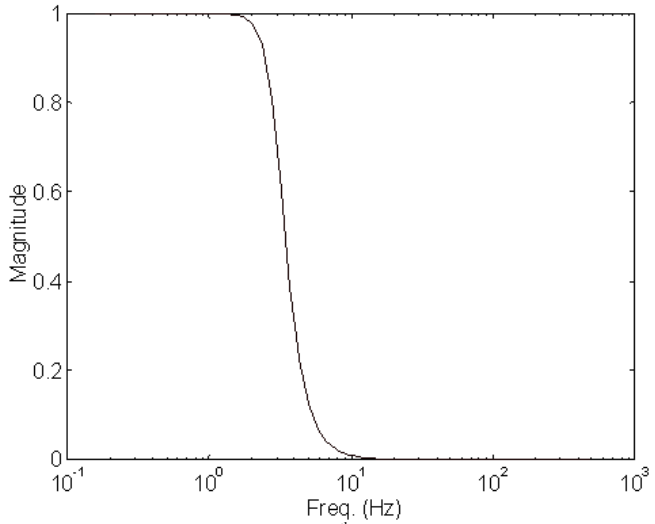

Fig. 12. The frequency response of a 4th-order low-pass filter.

E. The compensation filter design

Fig. 13 shows the frequency response of the perturbation function $P_e(z^{-1})$. Because the 4th-order low-pass filter $LPF(z^{-1})$ as in (11) significantly reduces the perturbation caused by modeling error, the compensation filter $\Omega(z^{-1})$ is omitted.

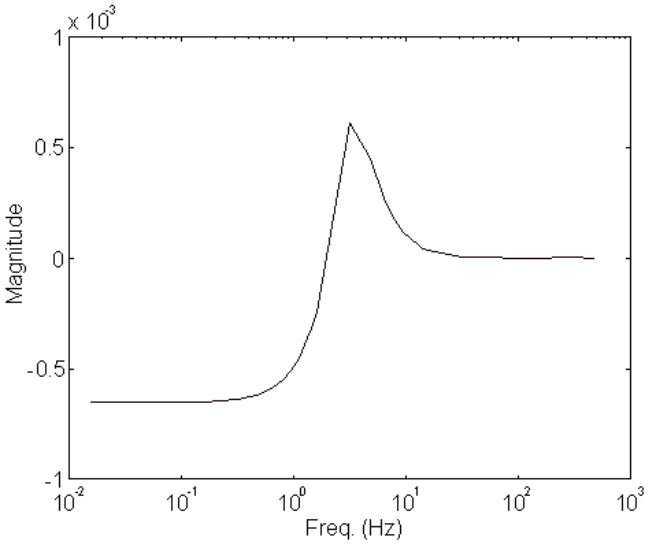

Fig. 13. The frequency response of perturbation function.

F. The speed perturbation caused by reaction torque

For testing the performance of speed perturbation observer, a force task is performed on the mechanical system as shown in Fig. 8. Fig. 14 and Fig. 15 show the experimental results of the axial mechanical system with different control laws.

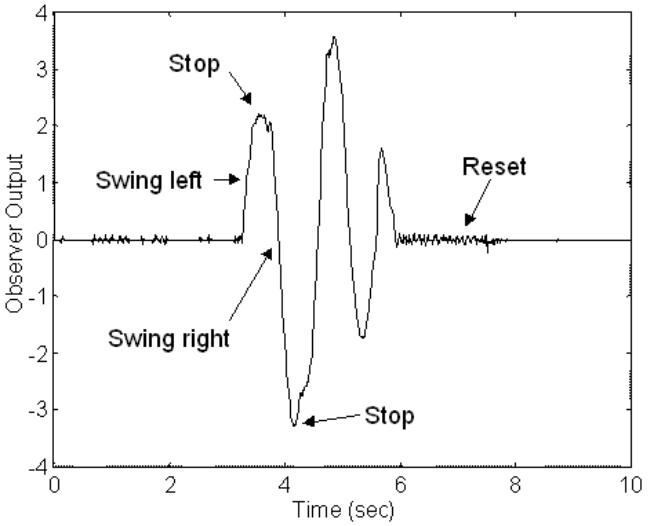

Fig. 14. The speed perturbation caused by reaction torque.

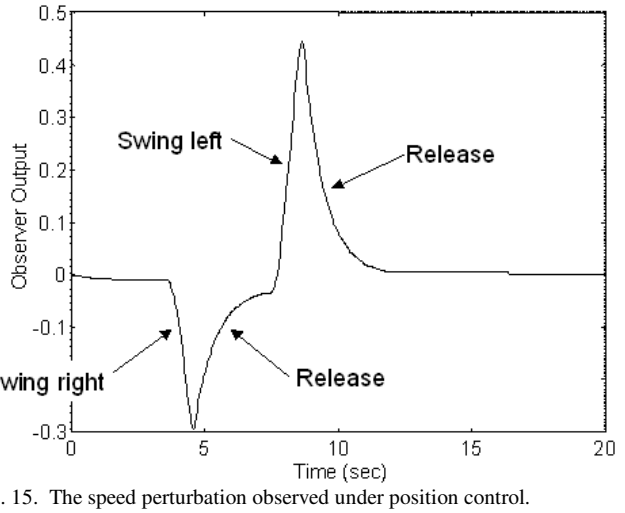

Fig. 15. The speed perturbation observed under position control.

The reaction torque is applied to the mechanical system by swing the handler. Fig. 14 shows the experimental result of

the torque controlled axial mechanical system. The observer quickly responses the speed variation caused by reaction torque. Fig. 15 shows the experimental result of the position controlled axial mechanical system. The damping responses are observed when the handler is released after swing operation.

V. Experimental Results: An Ink-Jet Printer

The experimental setup of an ink-jet printer for the present study is shown in Fig. 16. The applied experiment system consists of a DSP controller and an ink-jet printer. The DSP controller has built-in a high-performance TI TMS320F2812 digital signal controller, which is capable of implementing control laws at a sampling period of 1 ms. The ink-jet printer consists of a DC motor, a gear set, and some rollers to transmit paper from the lower paper tray to another paper tray. In this paper, the DC motor is controlled by the DSP controller for testing the proposed approach.

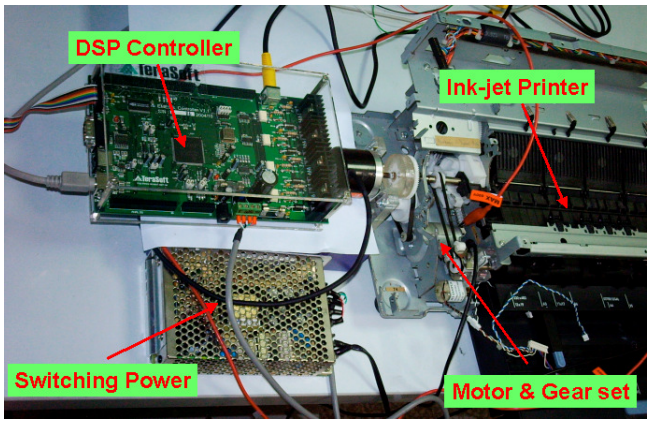

Fig. 16. The experimental setup of an ink-jet printer.

In experiments, the observer shown in Fig. 1 is used to estimate the speed perturbation caused by external disturbances that are induced by different paper path situations such as paper sticking, paper jamming, paper slipping, parts cracking, parts chattering, and parts wearing. In this study, only the speed perturbation induced by specific paper path situation is the main concern in the ink-jet printer. For instance, the estimation of the speed perturbation caused by parts cracking could be used to index a serious situation in the ink-jet printer. Fig. 17 shows the structure of the identification unit developed in this study. By using the filtered perturbation signal $\hat{d}^*(t)$, the identification unit with feature extraction and comparison is applied to distinguish the speed perturbation caused by specific torque disturbance. Here, the different torque disturbances are mainly caused by the different paper path situations. For instance, $F_{\text{sticking}}{}^*(t)$, $F_{\text{jamming}}{}^*(t)$, $F_{\text{cracking}}{}^*(t)$, and $F_{\text{chattering}}{}^*(t)$ denote the sampled load torques caused by paper sticking, paper jamming, parts cracking, and parts chattering, respectively. There are two phases for designing the identification unit. In the first phase, by applying the speed perturbation observer as shown in Fig. 1, some features are extracted from the filtered perturbation signal $\hat{d}^*(t)$. Then, the extracted features are stored in database for further applications. For instance, if paper jamming occurs in paper feeding processes, the signal $\hat{d}^*(t)$ will rise to a larger value than that estimated under normal conditions. The magnitude of the filtered perturbation signal $\hat{d}^*(t)$ is therefore an important feature in applications. After taking several experiments, features with different paper path situations are obtained and stored in the database as shown in Fig. 17. The second phase is applied for on-line identifying and indexing different paper path situations. As shown in Fig. 17, the identification unit extracts features from the filtered perturbation signal $\hat{d}^*(t)$, and then compares with the features stored in database. Therefore, a specific paper path situation can be successfully identified if the on-line extracted features are similar to those stored in database. For instance, the identification unit indexes paper jamming situation if the on-line extracted features are similar to those obtained by paper jamming experiment.

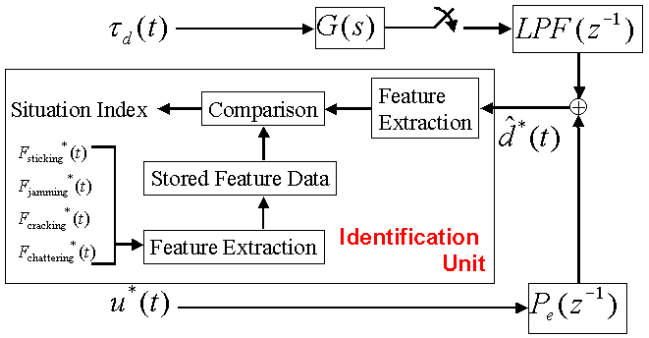

Fig. 17. Identification unit with feature extraction and comparison.

For testing the performances of the proposed approach, two usual paper path situations, paper jamming and mechanical chattering, are tested on the experiment system as shown in Fig. 16. According to the frequency analysis, a 4th-order low-pass filter with bandwidth 3.25 rad/sec is designed as

$$LPF(z^{-1}) = \frac{\begin{pmatrix} 0.5845 + 2.3381z^{-1} + 3.5071z^{-2} \\ +2.3381z^{-3} + 0.5845z^{-4} \end{pmatrix} \times 10^{-7}}{\begin{pmatrix} 1 - 3.9179z^{-1} + 5.7571z^{-2} \\ -3.7603z^{-3} + 0.9212z^{-4} \end{pmatrix}} \qquad (12)$$

Fig. 18 shows the experimental results for detecting paper jamming situation. Clearly, the observer accurately responses paper jamming situation at 3 seconds after starting printing process. The response time that depends on the low-pass filter design is about 1 second. In the experiment, the magnitude of the filtered perturbation signal $\hat{d}^*(t)$ is an important feature. Normally, without paper jamming, the magnitude of the signal $\hat{d}^*(t)$ is within 10 units. However, the magnitude is increased to approximately 120 units when the paper jamming situation occurs. Thus, the magnitude with 10 units can be a feature for indexing paper jamming situation. Although an overshoot occurs as shown in Fig. 18, it does not affect the detection result for paper jamming situation.

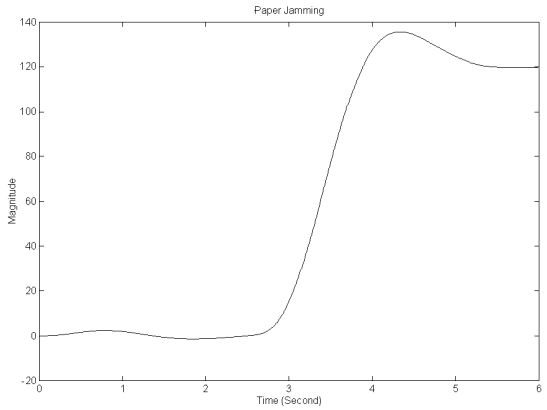

Fig. 18. The speed perturbation caused by paper jamming.

Fig. 19 shows the experimental results for detecting mechanical chattering situation. Clearly, the observer accurately responses the mechanical chattering situation at 3 seconds after starting printing process. The response time is about 1 second. In comparing with Fig. 18, the filtered perturbation signal $\hat{d}^*(t)$ with different waveforms can denote different paper path situations. As shown in Fig. 19, not only the magnitude of the signal $\hat{d}^*(t)$ is increased to approximately 60 units, but also some fluctuations are detected when mechanical chattering situation occurs. Therefore, the magnitude and the fluctuations of the filtered perturbation signal $\hat{d}^*(t)$ are both the important features in applications. In the experiment, as shown in Fig. 19, the observer indexes mechanical chattering situation when the magnitude of the signal $\hat{d}^*(t)$ is over 10 units and the number of fluctuations is over 5 times.

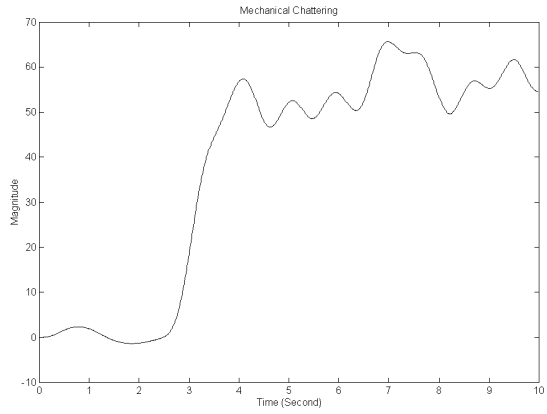

Fig. 19. The speed perturbation caused by parts chattering.

VI. Conclusion

Because paper transmission problems usually occur for a long period using an ink-jet printer, the detection of paper path situations is thus required for ensuring printing qualities and for preventing destructive damages. Although many researchers have proposed several advanced detection methods, a simple detection method with few sensors is still preferred in most applications by considering the production cost of an ink-jet printer. However, the paper path detection method with few sensors usually limits detection performances because few sensors only provide little information about paper path situations during paper feeding processes. Therefore, it is interesting to design a detection method that can detect some paper path situations without additional sensors. In this paper, the speed perturbation observer is proposed to detect paper path situations in an ink-jet printer. In comparing with the existing approaches, the proposed approach detects several paper path situations without additional sensors. Moreover, in comparing with the torque disturbance observer, the speed perturbation observer is less sensitive to measurement noise and modeling error, and can provide stable computation in digital control systems. By applying feature extraction and comparison methods, an identification unit is included for identifying specific paper path situations in an ink-jet printer. Experimental results demonstrate that the proposed approach provides good detection results and is feasible for detecting specific paper path situations in ink-jet printers.

References

[1] C. Kim and D. Cha, "Simulation of paper transport to design the paper path of a LBP," in *Proceedings of the International Conference on Digital Printing Technologies*, vol. 2004, pp. 189-193, 2004.

[2] D. Y. Koo, S. H. Han, and S. H. Lee, "An object-oriented configuration design method for paper feeding mechanisms," *Expert Systems with Applications*, vol. 14, no. 3, pp. 283-289, 1998.

[3] B. Bukkems, R. Van De Molengraft, M. Heemels, N. Van De Wouw, and M. Steinbuch, "A piecewise linear approach towards sheet control in a printer paper path," in *Proceedings of the American Control Conference*, vol. 2006, pp. 1315-1320, 2006.

[4] R. Sanchez, R. Horowitz, and M. Tomizuka, "Paper sheet control using steerable nips," in *Proceedings of the American Control Conference*, vol. 1, pp. 482-487, 2004.

[5] M. Krucinski, C. Cloet, M. Tomizuka, and R. Horowitz, "Asynchronous observer for a copier paper path," in *Proceedings of the IEEE Conference on Decision and Control*, vol. 3, pp. 2611-2612, 1998.

[6] F. Zhao, X. Koutsoukos, H. Haussecker, J. Reich, and P. Cheung, "Monitoring and fault diagnosis of hybrid systems," *IEEE Transactions on Systems, Man, and Cybernetics, Part B: Cybernetics*, vol. 35, no. 6, pp. 1225-1240, 2005.

[7] G. Fung, X. Z. Gao, and S. J. Ovaska, "Fault detection in ink jet printers using neural networks," in *Proceedings of the IEEE International Conference on Systems, Man and Cybernetics*, vol. 7, pp. 485-490, 2002.

[8] Y. Ishikawa, "Paper jam detector for electrophotograph printer," *U.S. PATENT* 5,713,059, 1998.

[9] M. Chen and C. Y. Chen, "Sheet feeder capable of immediately detecting a paper jam," *U.S. PATENT* 6,880,819, 2005.

[10] S. Katsura, Y. Matsumoto, and K. Ohnishi, "Realization of "law of action and reaction" by multilateral control," *IEEE Transactions on Industrial Electronics*, vol. 52, no. 5, pp. 1196-1205, October, 2005.

[11] S. Katsura, W. Iida, and K. Ohnishi, "Medical mechatronics - An application to haptic forceps," *Annual Reviews in Control*, vol. 29, no. 2, pp. 237-245, 2005.

[12] Y. Yasui, K. Shimojo, M. Saito, and H. Tamagawa, "Accurate engine speed control using adaptive disturbance observer," *Review of Automotive Engineering*, vol. 26, no. 2, pp. 137-141, April, 2005.

[13] Z. L. Liu and J. Svoboda, "A new control scheme for nonlinear systems with disturbances," *IEEE Transactions on Control Systems Technology*, vol. 14, no. 1, pp. 176-181, January, 2006.

[14] W. H. Chen, "Disturbance observer based control for nonlinear systems," *IEEE/ASME Transactions on Mechatronics*, vol. 9, no. 4, pp. 706-710, December, 2004.

[15] S. S. Yeh, Z. H. Tsai, and P. L. Hsu, "Applications of Integrated Motion Controllers for Precise CNC Machines," *International Journal of Advanced Manufacturing Technology*, vol. 44, no. 9-10, pp. 906-920, 2009.

[16] S. J. Kwon and W, K, Chung, "A discrete-time design and analysis of perturbation observer for motion control applications," *IEEE*

Transactions on Control Systems Technology, vol. 11, no. 3, pp. 399-407, May, 2003.

[17] M. Bertoluzzo, G. S. Buja, and E. Stampacchia, "Performance analysis of a high-bandwidth torque disturbance compensator," *IEEE/ASME Transactions on Mechatronics*, vol. 9, no. 4, pp. 653-660, December, 2004.

[18] T. Murakami, F. Yu, and K. Ohnishi, "Torque Sensorless Control in Multidegree-of-Freedom Manipulator," *IEEE Transactions on Industrial Electronics*, vol. 40, no. 2, pp. 259-265, April, 1993.

[19] K. H. Chen and S. S. Yeh, "Estimation of the Force-Interactive Behaviors between Human and Machine Using an Observer-Based Technique," Lecture Notes in Engineering and Computer Science: Proceedings of The International MultiConference of Engineers and Computer Scientists 2012, IMECS 2012, 14-16 March, 2012, Hong Kong, pp. 956-961.

[20] T. Söderström and P. Stoica, *System Identification*, New York: Prentice Hall, 1989

[21] S. S. Yeh and H. C. Su, "Development of Friction Identification Methods for Feed Drives of CNC Machine Tools," *International Journal of Advanced Manufacturing Technology*, vol. 52, no. 1-4, pp. 263-278, 2011.